Acetonitrile Adsorption and Adhesion Energies onto the Pt(111) Surface by Calorimetry

Griffin Ruehl^{†,1}, S. Elizabeth Harman^{†,2}, Líney Árnadóttir³, and Charles T. Campbell^{*,1,2}

¹Department of Chemical Engineering and ²Department of Chemistry, University of Washington, Seattle, Washington 98105-1700, United States

³School of Chemical, Biological, and Environmental Engineering, Oregon State University, Corvallis, Oregon 97331-2702, United States

- * Corresponding Author, charliec@uw.edu
- [†] These authors share first authorship.

Keywords: catalysis, electrocatalysis, adsorption calorimetry, adsorption energy, acetonitrile, platinum, solvent effects

Abstract

Acetonitrile is a common solvent for heterogeneous catalysis and electrochemical applications, as well as the simplest example of an organic nitrile. Understanding the energetics and nature of its interactions with Pt(111) is of interest for a wide array of applications, especially for estimating the effect of acetonitrile as a solvent on the adsorption energies of catalytic and electrocatalytic reaction intermediates on Pt group metals. Here, the heat of adsorption of molecular acetonitrile on clean Pt(111) was measured by single crystal adsorption calorimetry (SCAC) as a function of coverage, and from that, the adhesion energy of liquid acetonitrile to Pt(111) was estimated. At 180 K, the differential heat of adsorption is initially 82.9 kJ/mol, decreasing to 63.2 kJ/mol by a saturation coverage of 0.25 ML. The integral (average) heat of adsorption at 180 K is 74.3 kJ/mol at a saturation coverage of 0.25 ML. At 100 K, the heat of adsorption is 84.5 kJ/mol initially, and decreases to ~45 kJ/mol after the completion of the first layer (0.35 ML), and finally reaches a constant multilayer heat of 43.4 kJ/mol at coverages higher than 0.7 ML. (Errors bars on all heats are ±4%.) The saturation coverage is higher at 100 K than 180 K, attributed to the formation of a less stable adsorbate configuration at 100 K due to lower surface mobility. Using the heats of adsorption at 100 K up to bulk-like multilayer coverages, we estimate the adhesion energy for liquid acetonitrile to Pt(111) to be 0.198 J/m², which can be used to estimate the effect of acetonitrile as a solvent on the adsorption energies of catalytic reactants relative to gas phase. This adhesion energy is considerably lower than those for water, benzene, and phenol on Pt(111), but slightly greater than those for methanol and formic acid.

1. Introduction

Due to its wide use as a solvent, the interactions of acetonitrile with Pt surfaces are important in electrochemistry and electrocatalysis. As the simplest example of an organic nitrile, a fundamental understanding of its interactions with Pt(111) is also of general interest to surface chemistry and catalysis. Here we report calorimetric measurements of the adsorption energies versus coverage of molecularly adsorbed acetonitrile on clean Pt(111) at 100 K and 180 K, and estimate from these the adhesion energy of liquid acetonitrile to Pt(111) at room temperature. Most importantly, this adhesion energy can be used to estimate the adsorption energies of catalytic reaction intermediates on Pt(111) in an acetonitrile solvent based on energies measured (or calculated) in gas phase. This is done using an equation we recently developed which shows that the difference in adsorption energy in liquid solvent relative to gas phase is dominated by the product of this solvent adhesion energy times the footprint area of the adsorbed intermediate on the surface. 1,2 Since there is vast knowledge already of adsorption energies on Pt group metals in gas phase, but very few such energies known in liquid solvents, this opens up important new opportunities to gain fundamental insights into catalysis in liquid solvents and electrocatalysis.

Acetonitrile is a polar, organic solvent commonly used in a number of chemical reactions and synthesis processes. It's high dielectric constant and aprotic nature make it an attractive electrolyte solvent in electrochemical reactions and electrocatalysis, ^{3–8} as well as in batteries and capacitors. ^{9–13} It's low viscosity and high miscibility with a wide variety of polar solvents and solutes makes it promising for applications in many other areas of heterogeneous catalysis including bio-fuels synthesis and biomass based chemical upgrading, as well as the engineering of optimal mixed solvent environments. ^{14–18} The measurement here of its adhesion energy to a Pt-group metal, and the use of that value to estimate adsorption energies of catalytic and electrocatalytic reaction intermediates on that and other Pt-group metal surfaces, which generally have similar adsorption and adhesion energies to Pt^{19–21} will aid in developing basic understanding of those important reactions, their mechanisms, and their reaction energy diagrams.

Platinum, in addition to its widespread use as a heterogeneous catalyst in numerous industrial processes, is a common electrode material for electrochemical applications. Therefore, elucidating the energetics and nature of interaction between acetonitrile and the Pt surface is of great interest. Pt(111) is the most thermodynamically stable face of platinum, and is consequently commonly used as a model catalyst. Previously, experimental results from temperature programmed desorption (TPD) and vibrational spectroscopy (RAIRS) studies have shown that acetonitrile will form multilayers at low temperatures (<150 K), but only forms a single, molecularly adsorbed adlayer from 150 K to ~200 K.²² The adsorption of acetonitrile on Pt(111) has also been studied by density functional theory (DFT).^{23–25} Here, we report the enthalpies of adsorption for acetonitrile to clean Pt(111) at 100 K and 180 K, determined in ultrahigh vacuum conditions using single crystal adsorption calorimetry (SCAC). These results, when combined with those recent RAIRS, TPD, and DFT studies, provide detailed insight into

the nature and energy of surface adsorption and interaction of acetonitrile with Pt(111). Enthalpies of adsorption for acetonitrile to clean Pt(111) have also been studied by SCAC previously, but only at 298 K,²⁴ where later TPD studies show that the first layer is already desorbed almost completely.²² The highly accurate adsorption energy and estimated adhesion energy of acetonitrile on Pt(111) reported here are the first such values reported for any nitrile-containing molecule on any Pt-group metal surface, and as such they serve as important benchmarks for validating the energy accuracy of computational methods (like density functional theory) used to estimate these energies when nitrile groups are involved. In addition, a recently developed method by this group has enabled the extraction of solvent adhesion energies from SCAC measurements of adsorption energies in ultrahigh vacuum (UHV). 19 Below, we use this method to extract and report the adhesion energy of liquid acetonitrile to the Pt(111) surface. This adhesion energy can in turn be used to quantitatively estimate the effect of this important solvent on the adsorption energies of catalytic reaction intermediates, as described previously. 1,2 This knowledge is of interest for efforts to utilize solvent properties to tune intermediate energetics and interactions with the catalyst surface, and consequently affect reaction rates and selectivities in liquid solvents.

2. Experimental Methodology

The experiments were performed in an ultrahigh vacuum (UHV) chamber (base pressure < 2 x 10⁻¹⁰ mbar) designed for single crystal adsorption calorimetry (SCAC). The chamber is also equipped with X-ray photoelectron spectroscopy (XPS), low energy electron diffraction (LEED), Auger electron spectroscopy (AES), low energy ion scattering spectroscopy (LEIS), a quadrupole mass spectrometer (QMS), and a liquid-nitrogen-cooled quartz crystal microbalance (QCM). The SCAC apparatus and experimental procedures for the molecular beam flux, sticking probability, and heat measurements have been described in depth previously.^{26–28}

To briefly summarize, the Pt(111) sample used was a 1 μ m thick single-crystal foil provided by Bine Hansen at Aarhus University. The surface was cleaned by repeated cycles of Ar⁺ ion sputtering and annealing to 1120 K. The Pt(111) surface was exposed to a pulsed, collimated molecular beam of acetonitrile and the heat of adsorption and sticking probability were recorded simultaneously. The sticking probability was measured with a QMS using the King and Wells method,²⁹ and the heat of adsorption was measured by a pyroelectric ribbon pressed against the back of the Pt(111) crystal. The molecular beam was created by expanding approximately 1.5 mbar of acetonitrile through a glass capillary array and collimated through a series of orifices that are cooled with liquid nitrogen. The resulting molecular beam is then chopped into 102 ms pulses every 3 s.

Here, one monolayer of coverage is defined as the number of molecules of acetonitrile adsorbed to the surface per unit area, normalized to the density of Pt atoms on the (111) surface ($1.50 \times 10^{19} \text{ atoms/m}^2$). A typical dose is 0.005 ML ($\sim 1.0 \times 10^{12} \text{ molecules}$ within the beam diameter of $\sim 4 \text{ mm}$) per acetonitrile gas pulse.

3. Results

3.1 Sticking Probabilities

Figure 1 shows the average long-term (S_{∞}) and short-term (S_{102ms}) sticking probabilities versus coverage for acetonitrile adsorption on clean Pt(111) at 180 K. The long-term sticking probability is the probability that a gas molecule strikes the sample surface, sticks, and remains until the next gas pulse starts 3 s later. This is used to calculate the adsorbate coverage remaining at the start of the next gas pulse. The short-term sticking probability is the probability that a gas molecule strikes the sample surface, sticks, and remains at least throughout the time window of the heat measurement (i.e., the first 102 ms). This is used to calculate the number of moles of gas-phase reactant that contribute to the measured heat of adsorption.

At 180 K, the long-term and short-term sticking probabilities were indistinguishable below 0.23 ML. They both start at a probability of ~0.98 and decrease with coverage to ~0.88 by 0.23 ML. Past this coverage, the long-term sticking probability drops off rapidly, reaching zero by 0.25 ML, while the short-term sticking probability remains high (>0.80). This indicates that the adsorption of acetonitrile on Pt(111) saturates by a coverage of 0.25 ML at 180 K, however acetonitrile continues to transiently adsorb on that adlayer with a high probability but desorbs again completely (but slowly) before the next pulse starts 3 s later.

Accurate determination of the long-term sticking probabilities at 180 K and high coverage was complicated by adsorption and desorption of acetonitrile on the walls of the vacuum chamber. Molecules that did not adsorb left the Pt surface and adsorbed transiently on the chamber walls, with a residence time on the same scale of the 3 s pulse period. This resulted in a mass spectrometer signal that was a combination of the 'real' signal coming from molecules directly leaving the Pt surface, and the 'background' signal of molecules desorbing from the chamber walls. Accurately distinguishing between these two signals was impossible without using a simple assumption based on previous TPD measurements. Those TPD results showed that more than a single layer will not build up at 180 K,²² and therefore the long-term sticking probability must drop to zero upon saturation of the first layer at 180 K. We used this to more accurately estimate the background signal of the mass spectrometer, chosen such that the long-term sticking probability decreases to zero after saturation at 180 K. As seen in *Figure* 1, this steep drop occurs at a coverage of ~0.25 ML. This measured long-term sticking probability was then applied to the heat measurements to calculate accurate coverages.

At 100 K, the short-term sticking probability starts at 0.98 and increases to unity within <1% by 0.15 ML. The long-term sticking probability is the same as the short-term sticking probability within error bars (~1%) at all coverages. As this temperature is cold enough to form multilayers of acetonitrile on the Pt(111) surface, the sticking probabilities remain at unity through the formation of at least 5 multilayers.

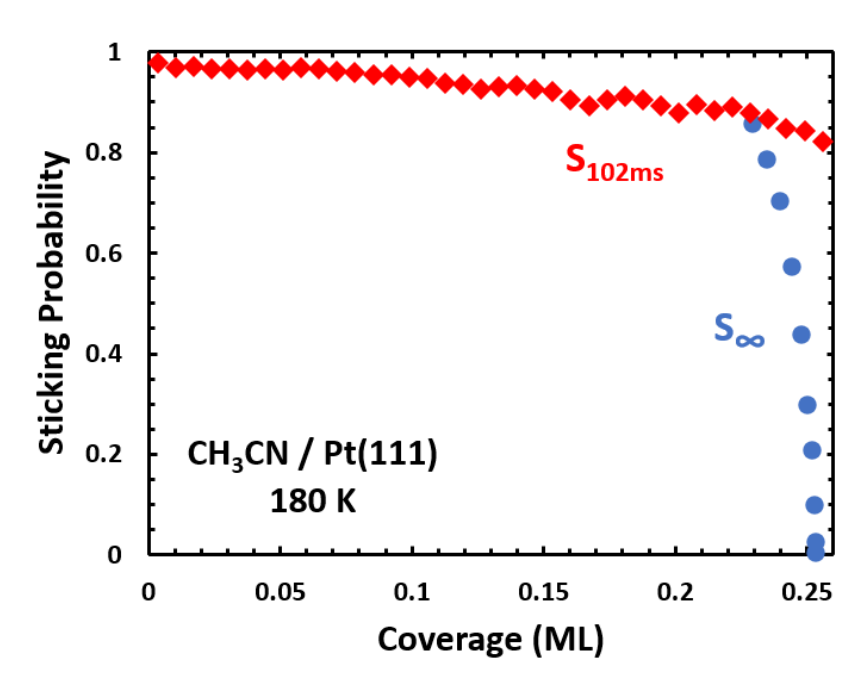


Figure 1: Average short-term (red, S_{102ms}) and long-term (blue, $S_{∞}$) sticking probabilities of acetonitrile on Pt(111) at 180 K as a function of acetonitrile coverage. A coverage of 1 ML is defined as 1 adsorbate per Pt(111) surface atom, or 1.50 x 10^{19} adsorbates/ m^2 . The short-term and long-term sticking probabilities were indistinguishable (within the noise) below 0.23 ML, so only one is shown.

3.2 Heats of Adsorption

In this paper, the term "heat of adsorption" is defined as the negative of the standard molar enthalpy change for the adsorption reaction, with the gas and the sample surface being at the same temperature. As explained in detail previously, this requires a small enthalpy correction on the measured heat since the gas molecule's enthalpy at this temperature is slightly different than a Boltzmann distribution at the sample temperature due to the actual experimental molecular beam conditions.²⁸ The differential heat of adsorption is the heat released per mole when a small increment of adsorbate is added to the surface at nearly fixed coverage, as occurs in one of our molecular beam pulses during SCAC. The integral heat of adsorption is the integral of the differential heat versus coverage from zero up to the coverage of interest, divided by that coverage, and is thus the average heat for that coverage range.

Figure 2 shows the differential heat of adsorption for acetonitrile on Pt(111) at 180 K (red) and 100 K (blue) (after this small correction to the raw heats) as a function of total acetonitrile coverage, along with the integral heat of adsorption at 180 K (black). These are the averages of 8 and 6 runs at 100 K and 180 K, respectively.

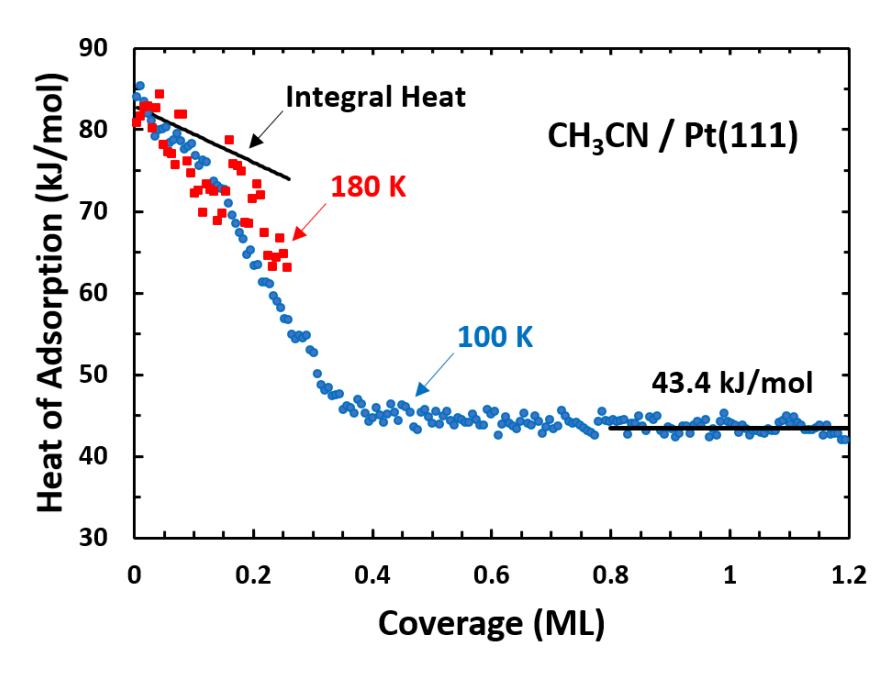


Figure 2: Differential heats of adsorption of acetonitrile on Pt(111) at 100 K (blue circles) & 180 K (red squares) as a function acetonitrile coverage. The average heat of adsorption reached at the multilayer limit is shown by the black line through the 100 K data. The integral heat of adsorption for 180 K is shown in black from the low coverage limit, fit by (82.9 - 34.40) kJ/mol and giving 74.3 kJ/mol at saturation (θ = 0.25 ML). 1 ML = 1.50 x 10^{19} molecules/m².

Previous results from literature show that acetonitrile molecularly adsorbs on Pt(111) below ~250 K, and multilayers will adsorb to the surface below 150 K.²² Thus, the calorimetric measurements here correspond to molecular adsorption on Pt(111), with multilayers of acetonitrile forming during the 100 K experiments but not at 180 K. The initial heat of adsorption at 100 K is 84.5 kJ/mol, which decreases until reaching ~45 kJ/mol by ~0.35 ML. The heat then remains constant through ~0.7 ML, before dropping slightly to a final multilayer heat of 43.4 ± 1.7 kJ/mol. (This is the run-to-run average and standard deviation of the multilayer heats of the 8 runs.) Each run's multilayer heat is the pulse-to-pulse average heat for coverages above 0.8 ML. This average multilayer heat is close to the heat of sublimation of bulk acetonitrile of 46.8 kJ/mol at 100 K, estimated from literature values for the enthalpies of phase transitions^{30,31} along with heat capacities of solid, liquid, and gaseous acetonitrile, 32 as a heat of sublimation at 100 K was not available in literature. Given the error bars in this estimate, the measured heat is probably within the combined error bars. This multilayer heat is also within the error bars of the value from the activation energy of desorption of 44 ± 3 kJ/mol calculated from TPD (discussed further below).²² The agreement with these values provides some estimation of the absolute accuracy of the results in Figure 2. This is consistent with our previous estimate of the accuracy of the absolute calibration of this calorimeter's heat measurement of 3%.20

The heat of adsorption at 180 K is initially 82.9 kJ/mol, decreasing to 63.2 kJ/mol by a coverage of ~0.25 ML. After this point the long-term sticking probability has dropped to zero, indicating that the monolayer of adsorbed acetonitrile has become saturated.

Any additional molecules that impinge on the surface adsorb transiently (as indicated by the high short-term sticking probability) but fully desorb before the start of the next pulse 3 s later. The integral heat of adsorption at 180 K is shown in black from the low coverage limit fit by $(82.9-34.4\theta)$ kJ/mol, where θ is coverage in ML, with a heat of 74.3 kJ/mol at saturation (0.25 ML).

We estimate the saturation coverage of the adsorbate layer at 180 K to be 0.25 ML. (The midpoint of the steep drop off in the long-term sticking probability in *Figure 1* occurs at 0.248 ML.) This is in excellent agreement with the coverage of ½ that corresponds to an ideal (2x2) overlayer with one acetonitrile molecule for every four Pt surface atoms. This is supported by a previous study that used low-energy electron diffraction (LEED) and found the presence of a (2x2) overlayer for acetonitrile adsorbed on Pt(111) up through coverages of 0.19 ML, though this pattern was replaced by an absence of long-range order by the next coverage studied of 0.36 ML and the experimental temperature was not reported.³³ Additionally, the Somorjai group found the acetonitrile saturation coverage on Ni(111) at 190 K to also be a (2x2) overlayer using LEED.³⁴ As seen in *Figure 2*, the first layer seems to complete at 100 K at a higher coverage, or ~0.35 ML.

Although the initial heat of adsorption is slightly higher at 100 K than at 180 K (84.5 vs. 82.9 kJ/mol), the difference is within the error bars associated with absolute heat calibration ($< \pm 4\%$) and thus the heat capacity is too small to measure accurately.

4. Discussion

4.1 Comparison to Temperature Programmed Desorption

Figure 3 compares the activation energy for desorption (E_{des}) of acetonitrile from Pt(111) versus acetonitrile coverage as determined from the heats measured here at 180 K from Figure 2 (black dots, corrected as needed by subtracting ½RT³⁵) to that from the TPD study of Tylinski et al.²² (The temperature T we used for this ½RT correction was 220 K, the mid-point of the monolayer TPD peak.) The smooth curve was determined by Tylinski et al. from the inversion of their TPD spectra for acetonitrile desorption from Pt(111) at different coverages, assuming the Polanyi-Wigner rate equation with a pre-factor of $v = 10^{16}$ s⁻¹ (which they assumed to be the same as that obtained from the Arrhenius fit of their multilayer desorption rates in TPD).

The bottom x-axis coverage (per Pt surface atom) here is defined relative to the surface density of Pt atoms on the (111) surface (1.50 x 10¹⁹ atoms/m²), as in *Figures 1-2*. The top x-axis coverage (ML_{Tylinski}) was defined by Tylinski *et al.* such that 1.0 ML_{Tylinski} is the highest coverage of acetonitrile before the multilayer peak first appears in the TPD spectra after dosing at 20 K. (One can see this was their definition of "ML" by inspection of the TPD spectra in *Figure 2* of their paper.) Even though the submonolayer peak is near saturation at that coverage, it is clear from careful inspection that it continues to grow at higher coverages, so that the first layer is not complete until a higher coverage than 1.0 ML_{Tylinski}. Instead, it seems more logical that in that study, the first layer completed at the midpoint of the 10-15 kJ/mol drop in E_{des} with coverage they reported at 1.2-1.5 ML_{Tylinski}. As shown above, the first layer completes at a coverage of ~0.25 acetonitrile molecules per Pt surface atom. We have thus adjusted

the coverage axes in the two curves in *Figure 3* such that 1.28 ML_{Tylinski} corresponds to 0.25 acetonitrile molecules per Pt surface atom.

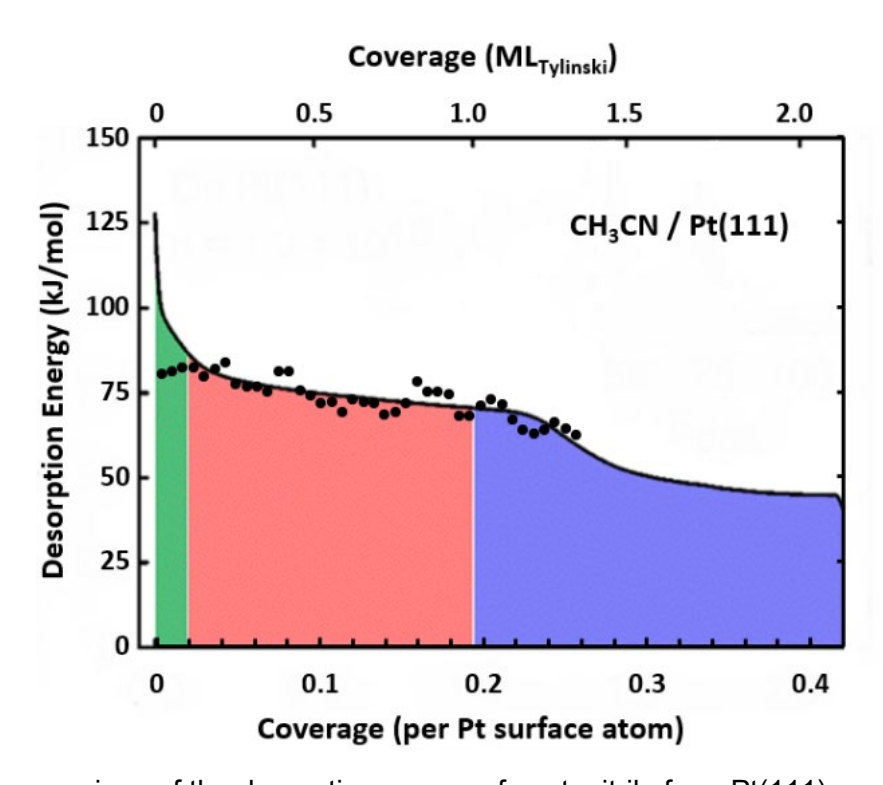


Figure 3: A comparison of the desorption energy of acetonitrile from Pt(111) as a function of acetonitrile coverage as determined from the differential heats measured in this work (black points) to the values determined by Tylinski *et al.*²² in a very careful TPD study (solid curve). The bottom x-axis coverage is defined as in *Figures 1 & 2*, i.e. relative to the density of Pt atoms on the (111) surface (1.50 x 10¹⁹ atoms/m²), while the top x-axis is in units as defined by Tylinski *et al.*, where 1 ML_{Tylinski} was the highest coverage of acetonitrile that showed no multilayer desorption peak in TPD. In this plot, we adjusted 1.0 ML_{Tylinski} to correspond to 0.195 ML (per Pt surface atom) to align the steepest (broadened step-like) drop in desorption energy versus coverage in Tylinski's data with the saturation coverage at 180 K (black points), which we assumed here to correspond to completion of the first layer of adsorbed acetonitrile at 0.25 ML (see text). The green, red, and blue shadings are from Tylinski *et al.* and were intended to separate the regions where TPD features were seen associated with step sites, (111) terraces in the first layer, and coverages where the multilayer TPD peak was also seen, respectively. We note that the TPD peak area associated with terrace sites continued to grow considerably in this blue region, which explains why 1.0 ML_{Tylinski} corresponds to a lower coverage than 0.25 ML.

As seen, with this adjustment the desorption energies versus coverage from the calorimetry results are in excellent agreement with those determined by TPD. The discrepancy at very low coverages is likely due to a higher concentration of surface defects (step sites) for the Pt(111) surface used for TPD than that used for calorimetry. Further, the multilayer heat of 43.4 ± 1.7 kJ/mol obtained from calorimetry is within the error bars of the activation energy of 44 ± 3 kJ/mol determined by Tylinski *et al.* from leading-edge analysis of the multilayer desorption peak (which can be corrected to a

heat of adsorption by adding ½RT = 0.47 kJ/mol with T = 140 K). The strong agreement of these results provides a convincing confirmation of each study. Collectively, the combination of energetic data from calorimetry and structural information from RAIRS performed by Tylinski *et al.* provides detailed insight into the nature and energy of surface adsorption and interaction of acetonitrile with Pt(111).

The adsorption of acetonitrile on Pt(111) was studied previously by SCAC, but only at 298 K by Shayegi *et al.*²⁴ The initial heat of adsorption reported there at 298 K (87 kJ/mol) is very close to that measured here at 100 K and 180 K in *Figure 2* (83-85 kJ/mol). However, the heat drops much more rapidly with coverage in those results at 298 K, and the saturation coverage (~0.18 ML) is lower. It is very clear from looking at the TPD spectra for acetonitrile on Pt(111) presented in *Tylinski et al.*²² that most of the first layer of molecularly adsorbed acetonitrile desorbs well below 298 K, so it is not clear what species Shayegi *et al.* were producing above ~0.05 ML. That SCAC study at 298 K²⁴ did not present the long-term and short-term sticking probabilities versus coverage, so it is difficult to assess how to interpret those data.

4.2 Monolayer Saturation Coverages

In the heats of *Figure* 2, saturation of the first layer appears to occur much later in the 100 K data, at a coverage of ~0.35 ML, than at 180 K (0.25 ML). This can be explained by a closer analysis of the acetonitrile adsorbate configurations, along with the lower surface mobility at 100 K which limits the ability for adsorbed molecules to arrange themselves in the most energetically stable configurations compared to those at 180 K. This also explains why the heat from ~0.2 to 0.25 ML is lower at 100 K than at 180 K in *Figure* 2.

Previous work using RAIRS, 3,22,36 EELS, 37 and computational methods 23-25 showed that the most stable orientation of the adsorbed acetonitrile molecule on Pt(111) is a bridged structure, referred to as the μ-configuration. This configuration was observed at temperatures as low as 60 K, but is the dominant surface configuration observed above 110 K in vacuum.²² In this configuration the C≡N triple bond becomes a C=N double bond, and new C-Pt and N-Pt bonds are formed, leaving the methyl group oriented away from the surface. Further, DFT calculations^{23–25} suggest that the second most stable orientation, referred to as the N-top configuration, is bound to a single Pt surface atom via the lone pair on the N atom, with the acetonitrile molecule oriented perpendicularly to the plane of the surface. The N-top configuration thus requires a smaller area on the surface than the μ-configuration. The N-top configuration was observed from 60-110 K by RAIRS, but was only present above 110 K in vacuum at coverages nearing and above saturation of the first layer (above 1 ML_{Tylinski}, or 0.19 ML per Pt surface atom).²² At the highest temperature they studied by RAIRS below 110 K (i.e. 60 K) there is not enough thermal energy for the adsorbates to overcome the activation barrier for the formation of the μ-configuration, and by coverages nearing the completion of the first layer, stearic constraints are present.²² Additionally, SFG measurements for acetonitrile in the liquid phase at a Pt electrode interface also observed the formation of the N-top configuration due to stearic constraints introduced by the presence of solvents (ethanol, methanol, or water).^{4,38}

At 100 K in UHV, all incoming acetonitrile molecules adsorb when they hit the surface, regardless of the local surface coverage where they hit, as evidenced by the unity sticking probability at high coverage. The heat stays much higher than in the second layer up to at least 0.25 ML (Figure 2), implying that they transiently adsorb when landing on top of preexisting adsorbates, and diffuse rapidly to find an adsorbatefree site to bind strongly to the Pt atoms below, as commonly occurs when organic molecules adsorb on late transition metal surfaces.³⁹ As the first absorbate layer nears saturation, stearic constraints arise which inhibit the formation of the μ-configuration, which requires multiple adjacent, unoccupied Pt surface atoms. This surface temperature is apparently cold enough to both prevent desorption as well as prevent the μ-bonded molecules from moving apart to create larger free metal sites to accommodate the more favorable µ-configuration. So, some molecules only have enough space to form the N-top configuration. The resulting surface adlayer is a combination of the µ and N-top configurations, enabling the formation of a higherdensity first layer that saturates by ~0.35 ML. This is consistent with RAIRS data showing the presence of both configurations on Pt(111) at 120 K at coverages near and above saturation of the first laver.²²

In contrast, the saturation coverage at 180 K is only 0.25 ML. As the first layer nears saturation at 180 K, any incoming adsorbate molecules that land at a less favorable site can migrate to a more favorable site or wait until thermal fluctuations create more open space to allow it to convert to the most stable μ-configuration. Again, RAIRS data observed the formation of the N-top configuration only below 110 K or at coverages higher than a single layer, but never at 180 K, which is too hot to form more than a single layer.²² Thus, thermal motion at 180 K enables the formation of an absorbate layer dominated by the more stable µ-configuration, as seen in literature for adlayers deposited over the range of 120-140 K.²² This results in a less densely packed first layer that saturates by 0.25 ML, but also makes the higher temperature (180 K) results in Figure 2 a more accurate approximation of the most stable structure of the first layer and its heat versus coverage. DFT calculations have shown that the μ -configuration is stable at a coverage of 0.25 ML (i.e., one per 2x2 unit cell), 23-25 consistent with the saturation coverage we measure here at 180 K of 0.25 ML. This is further supported by LEED studies that have observed a (2x2) overlayer structure for acetonitrile adsorbed on Pt(111) and Ni(111). On Pt(111) the (2x2) overlayer was observed up through coverages of 0.19 ML, but was no longer present by a coverage of 0.36 ML.33 For Ni(111), the acetonitrile saturation coverage at 190 K was found to be a (2x2) overlayer.34

4.3 Adhesion Energy

Given how commonly acetonitrile is used as a solvent, determination of the adhesion energy of liquid acetonitrile on Pt(111) can provide valuable insight into the energetics of the liquid-solid interface. It has been shown that solvent-metal adhesion energies are the dominating factor that determines differences in reactant adsorption energies in different solvents or in any solvent relative to gas-phase adsorption energy measurements.^{1,19} Solvent adhesion energies allow one to quantitatively estimate the effects of different solvents on the adsorption energies of catalytic reaction intermediates.¹ Thus, it is highly desirable to measure the adhesion energy of

acetonitrile to Pt(111) to enable the prediction of adsorption energies of molecules to Pt(111) in an acetonitrile solvent. However, there is currently no way to directly measure the adhesion energy of a liquid solvent to a clean metal surface.

To estimate this adhesion energy, we will employ a recently developed method from this group. 1,19 This method used a standard thermodynamic cycle to derive a relationship between the adhesion energy of a solvent and the experimentally determined differential heat of adsorption data like that in *Figure 2*. Notably, this requires heat versus coverage measurements out to multilayer coverages of the solid solvent and that the coverage has known absolute units. This derived relationship is presented in *Equation 1*, where $E_{adh,S(liq)/M(s)}$ is the adhesion energy of the liquid solvent to the solid metal, and $\gamma_{S(liq)}$ is the surface energy of the liquid solvent at its gas or vacuum interface: 19

$$E_{adh,S(liq)/M(s)} = [Q_{adsorption} - n \cdot \Delta H_{vap,S}]/A + 2 \cdot \gamma_{S(liq)}$$
 (1)

As shown in this derivation, 19 $\gamma_{S(liq)}$ is multiplied by 2 here because, in the thermodynamic cycle used there, the first step is to produce (from gas molecules) a free-standing liquid slab, whose energy is higher than bulk-like liquid by $\gamma_{S(liq)}$ times the area of both the top and the bottom surfaces of the slab. The term $[Q_{adsorption} - n \cdot \Delta H_{vap,S}]/A$ here is equal to the integrated area from zero coverage up to a (bulk-like) multilayer coverage (with n moles adsorbed per area A) of the heatversus-coverage curve $(Q_{adsorption})$ minus n/A times the molar heat of vaporization of the liquid solvent ($\Delta H_{vap,S}$). Ideally, these values would all be measured at room temperature to provide the adhesion energy at room temperature. Since Qadsorption can only be measured on a clean metal surface in ultrahigh vacuum, which is only possible for acetonitrile at temperatures where the solvent grows as solid films rather than liquid films, the assumption was made that the term $\left[Q_{adsorption} - n \cdot \Delta H_{vap,S}\right]\!/A$ at room temperature is approximately equal to the analogous quantity at experimental temperatures where the solvent is a solid, or $\left[Q_{adsorption} - n \cdot \Delta H_{sub,S}\right]$ /A, where $\Delta H_{sub,S}$ is the heat of sublimation of bulk acetonitrile. (See references^{1,19} for justification of this assumption). We evaluate this quantity from the heat data in Figure 2 at 100 K as its integrated area above the solid horizontal line shown (at the bulk heat of sublimation). This is equivalent to assuming that the difference in the heat capacities (including the heat of fusion) between the first and subsequent layers of acetonitrile is negligible when heating from 100 K to 300 K.

Using this method and the reported surface tension of bulk, liquid acetonitrile of $\gamma_{S(liq)}$ = 0.02866 J/m², 40 we calculate the adhesion energy of liquid acetonitrile to the Pt(111) surface at 100 K to be E_{adh} = 0.198 J/m². Comparatively, this value is slightly greater than the adhesion energies of formic acid and methanol to Pt(111) (0.162 J/m² & 0.168 J/m², respectively) but considerably below that of water, benzene, and phenol (0.273 J/m², 0.447 J/m², & 0.468 J/m², respectively).¹¹ Understanding this adhesion energy, and particularly how it compares to other common solvents, contributes to the growing interest in using these solvents, or mixtures thereof, to tune reaction environments to have more desirable energetics for surface adsorption or desorption for

catalytic reactants and intermediates. We note that these adhesion energies were all estimated using the same assumption of a negligible difference in heat capacities (including the heat of fusion) between the first and subsequent layers, and the errors associated with this assumption are possibly large (~25%). However, all these errors are probably qualitatively similar, so these trends in E_{adh} values will remain. It is expected that computational approaches could provide estimates of the corrections needed for this heat capacity approximation.

We next show that this acetonitrile / Pt(111) adhesion energy can be used to estimate the adsorption energy of uncharged adsorbed catalytic reaction intermediates on Pt(111) in liquid acetonitrile solvent based on their far better-known values in the gas phase. The adsorption energy in acetonitrile is approximately equal to the gas-phase adsorption energy minus this adhesion energy times the area occupied on the surface per mole of the adsorbate. This is based on a bond-additivity type model which was used recently to derive a relationship between the adsorption energy of an adsorbate in gas phase and the adsorption energy of that adsorbate in a liquid solvent. Utilizing a thermodynamic cycle, a constant was derived to quantify the difference in these adsorption energies as a result of the presence of a solvent. This model was originally only for flat adsorbates (like benzene and phenol), but it was recently extended to adsorbates of arbitrary shape. This relationship is presented below in *Equation 2*, where $\Delta U_{ads,R(solvent)}$ is the adsorption energy of the adsorbate in solvent, $\Delta U_{ads,R(gas)}$ is its adsorption energy in gas phase, and the remaining bracketed term is the constant:

$$\Delta U_{ads,R(solvent)} = \Delta U_{ads,R(gas)} + \left[E_{adh,S/M} - \frac{\Delta U_{solvation,R(gas)}}{\sigma_{tot}} - \gamma_{S(liq)} \right] \sigma_{R} \tag{2}$$

The difference in adsorption energy is composed of the adhesion energy of the solvent to the surface (E_{adh.S/M}), the gaseous adsorbate's solvation energy per unit molecular area ($\Delta U_{solvation,R(gas)}/\sigma_{tot}$), and the solvent's surface energy ($\gamma_{S(liq)}$), all multiplied by the footprint area of the adsorbate on the surface (σ_R) . This equation is independent of the shape of the adsorbate other than the fact that the shape determines the ratio of the total outer surface area of the adsorbate (σ_{tot}) and the footprint of the adsorbate on the surface upon adsorption (σ_R). This constant is dominated by the solvent adhesion energy term, as the remaining terms are smaller, opposite in sign, and nearly cancel. The errors on this estimated constant are probably rather large (up to 30%), but we expect that it will capture the trends with changing solvents and adsorbates reasonably well. The determination of the adhesion energy of acetonitrile on Pt(111) therefore allows for the quantification of this constant and consequently the effect of acetonitrile as a solvent on the adsorption energy of any adsorbing species on Pt(111) for which the gas phase adsorption energy is known. This model, combined with this adhesion energy, provides a powerful tool for improving the understanding and computational models for liquid phase reactions on Pt(111) that use acetonitrile as a solvent, and in combination with previously published values for other solvents and catalyst surfaces,^{2,19} liquid phase heterogeneous catalysis in general.

5. Conclusions

The energetics of molecular adsorption of acetonitrile on Pt(111) were measured by SCAC, as a function of coverage. At 180 K, the integral heat of adsorption is 74.3 kJ/mol at a saturation coverage of 0.25 ML, and well fit at lower coverages by (82.9 – 34.40) kJ/mol. At 180 K, the initial differential heat of adsorption is 82.9 kJ/mol, which decreases to 63.2 kJ/mol by 0.25 ML. At 100 K, the initial heat of adsorption is 84.5 kJ/mol, which decreases to ~45 kJ/mol at the completion of the first layer (0.35 ML), and finally drops to a multilayer heat of 43.4 kJ/mol above coverages of 0.7 ML. This difference in saturation coverage of the first layer at 100 K versus 180 K is a result of the formation of two different surface adsorbate configurations, μ and N-top, with the former being more energetically favorable but the latter arising in the presence of stearic constraints, which are present at 100 K due to lower adsorbate mobility across the surface. These present results agree well with recent TPD and RAIRS studies, and collectively these results provide a clear understanding of the nature of interaction between acetonitrile, the simplest organic nitrile, and Pt(111).

Using the 100 K heat of adsorption curve measured out to multilayer coverages, we estimate the adhesion energy for liquid acetonitrile to Pt(111) to be 0.198 J/m². This is slightly higher than that of formic acid and methanol to Pt(111), but considerably lower than that of water, benzene, and phenol. This adhesion energy is useful for estimating the effects of acetonitrile as a solvent on the adsorption energies of catalytic reaction intermediates of interest in liquid-phase catalytic and electrocatalytic reactions.

6. Acknowledgements

The authors acknowledge support for this work by the National Science Foundation under grant number CBET-2004757.

References

- 1. Singh, N. & Campbell, C. T. A Simple Bond-Additivity Model Explains Large Decreases in Heats of Adsorption in Solvents Versus Gas Phase: A Case Study with Phenol on Pt(111) in Water. ACS Catal. 9, 8116–8127 (2019).
- 2. Akinola, J., Campbell, C. T. & Singh, N. Effects of Solvents on Adsorption Energies: a General Bond-Additivity Model. *J. Phys. Chem. C* **125**, 24371–24380 (2021).
- 3. Villegas, I. & Weaver, M. J. Progressive cation solvation at Pt(111) model electrochemical interfaces in ultrahigh vacuum as probed by infrared spectroscopy and work-function measurements. *Electrochim. Acta* **41**, 661–673 (1996).
- 4. Baldelli, S., Mailhot, G., Ross, P., Shen, Y.-R. & Somorjai, G. A. Potential Dependent Orientation of Acetonitrile on Platinum (111) Electrode Surface Studied by Sum Frequency Generation. *J. Phys. Chem. B* **105**, 654–662 (2001).
- 5. Feng, G., Huang, J., Sumpter, B. G., Meunier, V. & Qiao, R. Structure and dynamics of electrical double layers in organic electrolytes. *Phys. Chem. Chem. Phys.* **12**, 5468–5479 (2010).

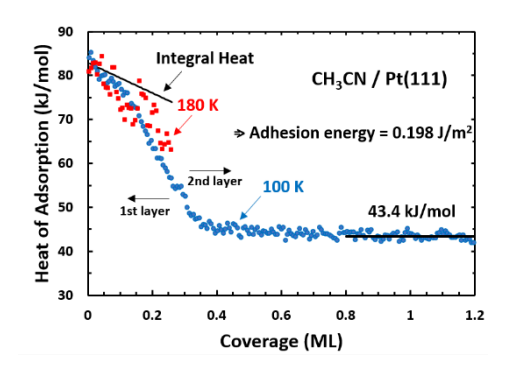
- 6. Pavlov, S. V & Kislenko, S. A. Effects of carbon surface topography on the electrode/electrolyte interface structure and relevance to Li–air batteries. *Phys. Chem. Chem. Phys.* **18**, 30830–30836 (2016).
- 7. Foley, J. K., Korzeniewski, C. & Pons, S. Anodic and cathodic reactions in acetonitrile / tetra-n-butylammonium tetrafluoroborate: an electrochemical and infrared spectroelectrochemical study. *Can. J. Chem.* **66**, 201–206 (1988).
- 8. Kiss, L. Electrooxidation of low-permittivity solvents in acetonitrile and solubility of trihexylamine in acetonitrile. *J. Iran. Chem. Soc.* **17**, 67–71 (2020).
- 9. Yamada, Y. *et al.* Unusual Stability of Acetonitrile-Based Superconcentrated Electrolytes for Fast-Charging Lithium-Ion Batteries. *J. Am. Chem. Soc.* **136**, 5039–5046 (2014).
- 10. Lane, G. H. & Jezek, E. Electrochemical studies of acetonitrile based supercapacitor electrolytes containing alkali and alkaline earth metal cations. *Electrochim. Acta* **150**, 173–187 (2014).
- 11. Zhang, S. *et al.* Insights into the effects of solvent properties in graphene based electric double-layer capacitors with organic electrolytes. *J. Power Sources* **334**, 162–169 (2016).
- 12. Trinh, N. D. *et al.* An Artificial Lithium Protective Layer that Enables the Use of Acetonitrile-Based Electrolytes in Lithium Metal Batteries. *Angew. Chemie Int. Ed.* **57**, 5072–5075 (2018).
- 13. Dou, Q. *et al.* Safe and high-rate supercapacitors based on an 'acetonitrile/water in salt' hybrid electrolyte. *Energy Environ. Sci.* **11**, 3212 (2018).
- 14. Zhang, Y. *et al.* Direct conversion of cellulose and raw biomass to acetonitrile by catalytic fast pyrolysis in ammonia. *Green Chem.* **21**, 812–820 (2019).
- 15. Mellmer, M. A. *et al.* Solvent-enabled control of reactivity for liquid-phase reactions of biomass-derived compounds. *Nat. Catal.* **1**, 199–207 (2018).
- 16. Walker, T. W. *et al.* Universal kinetic solvent effects in acid catalyzed reactions of biomass-derived oxygenates. *Energy Environ. Sci.* **11**, 617–628 (2018).
- 17. He, J. *et al.* Production of levoglucosenone and 5-hydroxymethylfurfural from cellulose in polar aprotic solvent-water mixtures. *Green Chem.* **19**, 3642–3653 (2017).
- 18. Kryachko, E. S. & Nguyen, M. T. Hydrogen Bonding between Phenol and Acetonitrile. *J. Phys. Chem. A* **106**, 4267–4271 (2002).
- 19. Rumptz, J. R. & Campbell, C. T. Adhesion Energies of Solvent Films to Pt(111) and Ni(111) Surfaces by Adsorption Calorimetry. *ACS Catal.* **9**, 11819–11825 (2019).
- 20. Campbell, C. T. Energies of Adsorbed Catalytic Intermediates on Transition Metal Surfaces: Calorimetric Measurements and Benchmarks for Theory. *Acc. Chem. Res.* **52**, 984–993 (2019).
- 21. Silbaugh, T. L. & Campbell, C. T. Energies of Formation Reactions Measured for Adsorbates on Late Transition Metal Surfaces. *J. Phys. Chem. C* **120**, 25161–25172 (2016).
- 22. Tylinski, M., Smith, R. S. & Kay, B. D. Structure and Desorption Kinetics of Acetonitrile Thin Films on Pt (111) and on Graphene on Pt (111). *J. Phys. Chem. C* **124**, 2521–2530 (2020).

- 23. Markovits, A. & Minot, C. Theoretical study of the acetonitrile flip-flop with the electric field orientation: adsorption on a Pt (111) electrode surface. *Catal. Letters* **91**, 225–234 (2003).
- 24. Shayeghi, A. *et al.* Adsorption of Acetonitrile, Benzene, and Benzonitrile on Pt(111): Single Crystal Adsorption Calorimetry and Density Functional Theory. *J. Phys. Chem. C* **121**, 21354–21363 (2017).
- 25. Pasti, I. A., Markovic, A., Gavrilov, N. & Mentus, S. V. Adsorption of Acetonitrile on Platinum and its Effects on Oxygen Reduction Reaction in Acidic Aqueous Solutions Combined Theoretical and Experimental Study. *Electrocatalysis* **7**, 235–248 (2016).
- 26. Ajo, H. M., Ihm, H., Moilanen, D. E. & Campbell, C. T. Calorimeter for adsorption energies of larger molecules on single crystal surfaces. *Rev. Sci. Instrum.* **75**, 4471–4480 (2004).
- 27. Lew, W., Lytken, O., Farmer, J. A., Crowe, M. C. & Campbell, C. T. Improved pyroelectric detectors for single crystal adsorption calorimetry from 100 to 350 K. *Rev. Sci. Instrum.* **81**, 1–9 (2010).
- 28. Lytken, O. *et al.* Energetics of Cyclohexene Adsorption and Reaction on Pt(111) by Low-Temperature Microcalorimetry. *J. Am. Chem. Soc.* **130**, 10247–10257 (2008).
- 29. King, D. A. & Wells, M. G. Molecular Beam Investigation of Adsorption Kinetics on Bulk Metal Targets: Nitrogen on Tungsten. *Surf. Sci.* **29**, 454–482 (1972).
- 30. Acree, Jr., W. E. & Chickos, J. S. Phase Transition Enthalpy Measurements of Organic and Organometallic Compounds. in *NIST Standard Reference Database Number 69* (eds. Linstrom, P. J. & Mallard, W. G.) (National Institute of Standards and Technology, 2021).
- 31. Domalski, E. S. & Hearing, E. D. Heat Capacities and Entropies of Organic Compounds in the Condensed Phase. Volume III. *J. Phys. Chem. Ref. Data* **25**, 1 (1996).
- 32. Yaws, C. L. Yaws' Handbook of Thermodynamic and Physical Properties of Chemical Compounds. (Knovel, 2003).
- 33. Garwood Jr., G. A. & Hubbard, A. T. Superlattices formed by interaction of polar solvents with Pt(111) surfaces studied by LEED, Auger spectroscopy and thermal desorption mass spectrometry. *Surf. Sci.* **118**, 223–247 (1982).
- 34. Gardin, D. E., Barbieri, A., Batteas, J. D., Van Hove, M. A. & Somorjai, G. A. Tensor LEED analysis of the Ni(111)-p(2x2)-CH3CN structure. *Surf. Sci.* **304**, 316–324 (1994).
- 35. Brown, W. A., Kose, R. & King, D. A. Femtomole Adsorption Calorimetry on Single-Crystal Surfaces. *Chem. Rev.* **98**, 797–831 (1998).
- 36. Ou, E. C., Young, P. A. & Norton, P. R. Interaction of acetonitrile with platinum (111): more properties of the n2(C,N) state and new species in the submonolayer. *Surf. Sci.* **277**, 123–131 (1992).
- 37. Sexton, B. A. & Avery, N. R. Coordination of acetonitrile (CH3CN) to Platinum (111): evidence for an n2 (C,N) species. *Surf. Sci.* **129**, 21–36 (1983).
- 38. Waldrup, S. B. & Williams, C. T. Acetonitrile Adsorption on Polycrystalline Platinum: An In Situ Investigation Using Sum Frequency Spectroscopy. *J. Phys. Chem. C* **112**, 219–226

(2008).

- 39. Chorkendorff, I. & Niemantsverdriet, J. W. *Concepts of Modern Catalysis and Kinetics*. (Wiley-VCH Verlag GmbH & Co. KGaA, 2007).
- 40. Haynes, W. M., Lide, D. R. & Bruno, T. J. CRC Handbook of Chemistry and Physics. (CRC Press, 2016).

TOC Graphic



For Table of Contents Only